

Preparation of *Ex Vivo*-Based Biomaterials Using Convective Flow Decellularization

Carolina Villegas Montoya, Ph.D., and Peter S. McFetridge, Ph.D.

With advantageous biomechanical properties, materials derived from *ex vivo* tissues are being actively investigated as scaffolds for tissue engineering applications. However, decellularization treatments are required before implantation to reduce the materials immune impact. The aim of these investigations was to assess a convective flow model as an enhanced methodology to decellularize *ex vivo* tissue. Isolated human umbilical veins were decellularized using two methods: rotary agitation at 100 rpm on orbital shaker plates, and convective flow run at 5, 50, and 150 mmHg within perfusion bioreactors. Extracted phospholipids and total soluble protein were assessed over time. Histology, SEM, and uniaxial tensile testing analysis were carried out to evaluate variation in the tissues. After 72 h, samples exposed to traditional rotary agitation showed retention of whole cells and cellular components, whereas pressure-based systems showed no visual sign of cells. The convective flow method was significantly more effective at removing phospholipid and total protein than the agitation model. High transmembrane pressure (150 mmHg) resulted in higher phospholipids extraction. However, a more efficient protein extraction occurred at 50 mmHg. Variation in extraction rates was dependent on tissue permeability, which varied as pressure increased. Collectively, these findings show significant improvements in decellularization efficiency that may lead to more immune compliant *ex vivo*-derived biomaterials.

Introduction

TISSUE ENGINEERING AIMS to treat injured or diseased tissues using 3D scaffolds to support cell growth and guide tissue regeneration. While many of these scaffolds are chemically synthesized, others are derived from natural *ex vivo* tissues; however, both must encourage cell infiltration and proliferation, as well as the establishment of a neo-blood supply. Simultaneously, scaffolds should provide sufficient mechanical strength to sustain physiological forces after implantation.¹ *Ex vivo* tissue remains a promising alternative to synthetic scaffolds; however, before implantation the tissue must be processed to extract cellular components that may elicit an immune response leading to the rejection of the implant.² *Ex vivo* materials, including acellular dermis, amniotic membrane, small intestinal submucosa, and heart valves, have been assessed as alternatives to synthetic matrices and have shown, overall, a positive host response, including angiogenesis, during regenerative events.¹

One of the challenges using *ex vivo* materials as implantable scaffolds is the removal of xeno- or allogenic cellular components while preserving the extracellular matrix (ECM). Decellularization involves the use of one or more agents to solubilize nonstructural ECM components allowing them to freely diffuse out of the tissue structure.³ Most research has

focused on specific chemistries or enzyme treatments to optimize the extraction of nonstructural tissue components, and have been extensively reviewed.^{2,4-7} The general approach used in current decellularization methods is to submerge the tissue in one or more treatment solutions and incubate either statically or expose the tissue to some form of agitation.⁸ These decellularization strategies are based mainly on passive diffusion, and commonly require extensive washing steps to not only strip the cellular fragments from the ECM, but also remove solvent residues. Decellularization efficiency is dependent on both tissue thickness and architecture, as the resistance to solvent diffusivity increases when samples are thicker or present a highly dense ECM.⁹ Further, current methods are likely to be less consistent due to nonuniform solvent delivery, as well as irregular folding or creasing through the agitation event.^{3,10,11} To obtain a cell free matrix, multiple decellularization agents maybe required (alcohols, surfactants, enzymes, etc.), as well as variation in their concentration and/or the time of exposure.³

Also important is the conservation of the ECM's mechanical properties, where aggressive compounds may damage structural components, or result in secondary effects such as removal of desired ECM components.^{1,2,9-12} Ionic detergents typically denature proteins leading to the

disruption of collagen integrity, while nonionic detergents reduce glycosaminoglycan, laminin, and fibronectin content.² Physical treatments such as sonication, snap freezing, and direct pressure can be used to assist decellularization both by disrupting cell membranes and rinsing the cellular material away. Others have used direct physical forces as a mechanism to isolate specific tissue sections from organs. The urinary bladder matrix is prepared using intraluminal water under pressure to facilitate the separation of the muscle layer from the tunica submucosa.¹³ The small intestinal submucosa is processed by physically removing the muscle layer and some portions of the mucosa, followed by chemical treatments to produce an acellular matrix.^{8,14,15} More recently, Karim *et al.*¹⁶ used a rotating perfusion bioreactor to decellularize and re-seed porcine heart valves, and Ott *et al.*¹⁷ decellularized whole rat hearts using a modified Langendorff apparatus.

In these investigations we have focused on the effect of the physical extraction mechanism, rather than the specific extraction chemistry, and as such have used an acetone/EtOH solution as a solubilizing agent. We describe the development of a novel decellularization system using modified vascular perfusion bioreactors and process flow circuits to produce an acellular biological matrix for tissue engineering applications. Dissected human umbilical veins (HUV) served as a model system to evaluate the effects of pressure-based decellularization. Bioreactors are typically designed to contain specific tissue types, and with simple modifications are suitable for decellularization purposes. A decellularization solution was perfused through the tube-side (lumen) of the vein to generate uniform convective, or radial flow, which was driven by the transmural pressure differential (see Fig. 1). The efficiency of phospholipid and protein extraction with pressure-based systems was evaluated and compared to traditional rotary agitation methods. By developing a versatile system that incorporates tissue decellularization, sterilization, cell seeding, and culture into a single system,

the risk of contamination and the time frame for construct maturation can be significantly reduced.

Materials and Methods

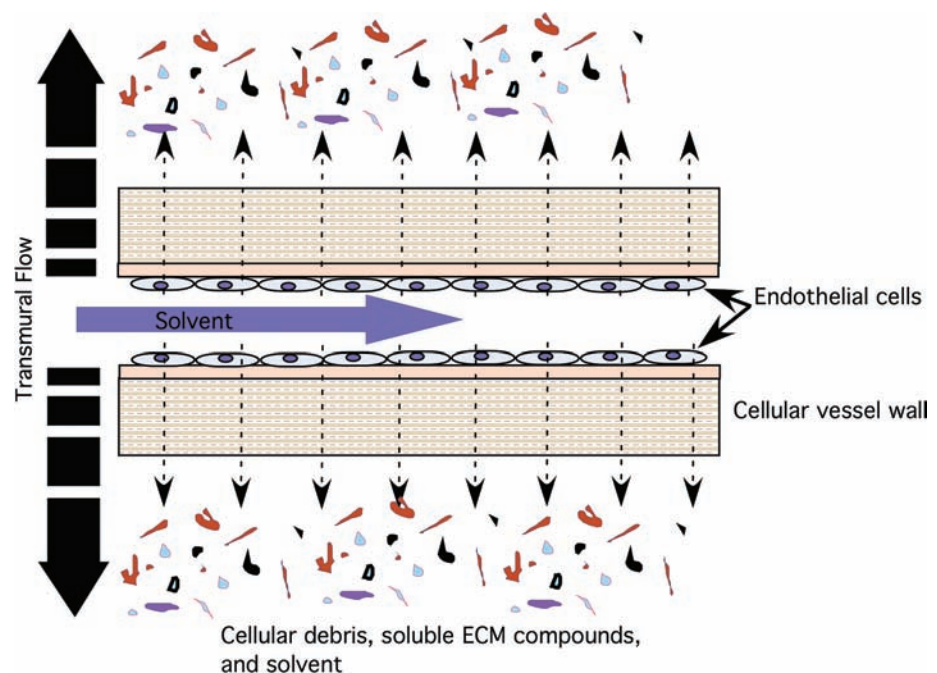
HUV isolation

HUV were isolated using an automated dissection method as previously described.¹⁸ Briefly, human umbilical cords were collected from a local hospital up to 48 h after delivery. Cords were then carefully rinsed with distilled water to remove residual blood and cut into 120-mm-long segments. Sections were then mounted on stainless steel mandrels (6 mm OD by 200 mm length) and fixed in place with nylon cable ties to maintain the vessels orientation during the freezing and dissection process. Mounted cords were placed in a sealed Styrofoam container and progressively frozen to -80°C , and maintained for at least 12 h to ensure a uniform temperature throughout the vessel wall. Mounted cords were then fixed between the headstock and the tailstock of a standard 10" bench lathe (model 33682; Harbour Freight, OK), and the cutting depth was adjusted to yield a 0.75 mm wall thickness. Rotational speed was set to 2900 rpm and the automatic drive set to an axial cutting rate of 5 mm/s. Immediately after dissection, veins were placed in the -20°C freezer for 2 h to allow them to gradually thaw and then were placed in the 5°C refrigerator before decellularization.

Agitation decellularization

Rotary agitation decellularization was carried out using dissected HUV segments 85 mm long with 5 mm ID and 6.5 mm OD. Samples were incubated in 100 mL of a solution composed of 20% acetone, 20% water, and 60% ethanol. Bottles (250 mL capacity) containing HUV samples were continuously agitated on an orbital shaker at 100 rpm for 72 h.

FIG. 1. Convective flow. Illustrated is the principle of convective flow driven by the lumen to ablumen pressure differential. The applied pressure enhances uniform cell lysis with the transmural flow acting as the carrier of soluble compounds out of the tissue scaffold. The process is further enhanced when a constant transmural flow of fresh solution moves across the membrane. Color images available online at www.liebertonline.com/ten.



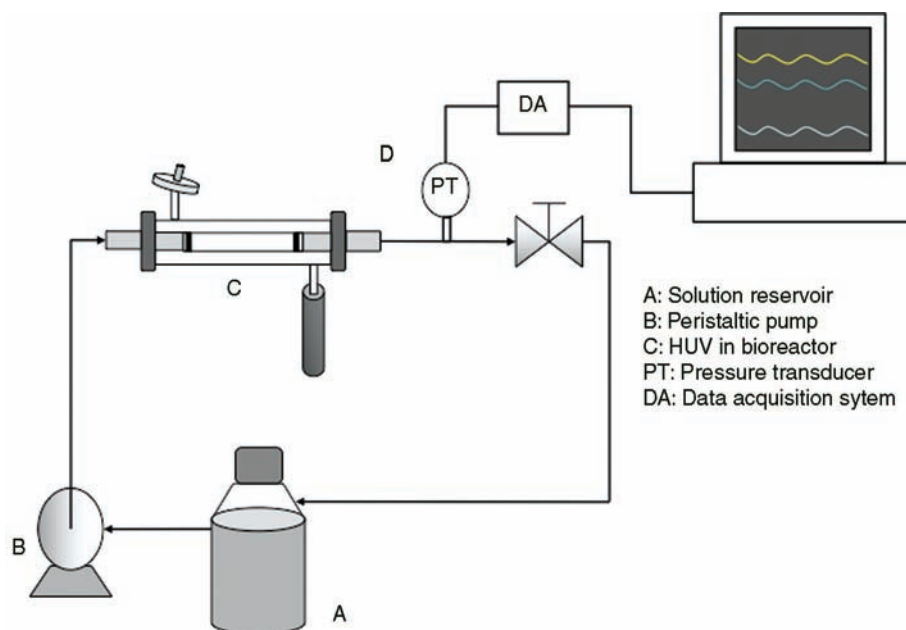


FIG. 2. Schematic representation of the convective flow decellularization apparatus. A peristaltic pump drives the solution through the tube-side (through the vessel lumen) at a constant flow rate of 50 mL/min. Pressure is measured immediately downstream of the bioreactor, and monitored continuously by the data acquisition system. The pulse generated by the peristaltic pump was reduced up to 90% using a pulse dampener located upstream the vessel. The one-way valve was selected according to the tested pressure (5, 50, or 150 mmHg). The volume of transmural flow was collected over time, and analyzed. Three independent systems were assessed for each pressure.

Convective flow decellularization

Figure 2 shows the experimental apparatus used for the convective flow decellularization. Before loading scaffolds into the bioreactor, tubular stainless steel adapters were inserted 5 mm into each end of the 85-mm-long vein segments and secured with cable ties to seal and ensure a discrete flow field through the vessel lumen. Three independent systems were used for each analysis ($n=3$), each one with 100 mL of the decellularization solution being continuously circulated. The assembly consisted of a main feed reservoir (250 mL), a peristaltic pump (L/S Digital Standard Drive, model 07523-60; Cole Parmer, IL), a perfusion bioreactor (12.9 mm ID and 80 mm long), a pressure transducer downstream from the bioreactor (PX-140; Omega, Stamford, CT), and a one-way check valve with a 1 psi cracking pressure (SS-4C-1; Swagelok, Norman, OK). An additional pulse dampener (LJ-07596-20; MasterFlex, Cole Parmer, IL) was incorporated into the system to minimize pulse effects produced by the peristaltic pump. The decellularization solvent was perfused at an average flow rate of 50 mL/min with pulse frequency of 2 Hz for all pressure conditions. The transmural pressure was acquired and monitored using Advantech control systems (PCL-818 and VisiDAQ PCLS-920-31/P; Advantech, CA). Three luminal pressures were evaluated for reduced-pulse flow: 5 ± 3 mmHg (CF-5), 50 ± 3 mmHg (CF-50), and 150 ± 3 mmHg (CF-150). For all the experiments, the flux produced by the convective flow was measured over a 72 h period and later combined with bulk flow for analysis.

Analysis of cellular markers

Collected decellularization solutions at the defined time points were evaporated (Rotavapor R-210/215; Buchi, Cole Parmer, IL) and then diluted in 5 mL of isopropanol. Phospholipids concentration was determined with the Phospholipid C kit (Wako Chemicals USA, Richmond, VA) by measuring the absorbance of the blue pigment at 600 nm, and the concentration was calculated following the protocol

supplied by the assay manufacturer. Total soluble protein was determined using the micro BCA protein Assay Reagent Kit (Pierce Biotechnology, Rockford, IL). After incubation, absorbance was measured at a wavelength of 550 nm and extracted proteins quantified using the standard protocol supplied with the assay kit.

Quantification of hydroxyproline

Hydroxyproline (HYP) was used as a marker for collagen degradation. HYP content was determined from the total flux over the 72 h period. Briefly, samples were hydrolyzed with a 6 M HCl solution at 120°C for 20 min, followed by the addition of 100 μ L 6 M NaOH. Chloramine-T reagent was added and incubated for 25 min at room temperature. An equal volume of Ehrlich's reagent (1 M *p*-dimethylaminobenzaldehyde in *n*-propanol/perchloric acid [2:1 v/v]) was added and incubated for 20 min at 65°C. Absorbance was measured at 550 nm. A mean value of Hyp per mg of dry tissue was used to calculate the percent relative to native tissue.¹⁹

Calculation of scaffold permeability

Membrane permeability was calculated for the convective decellularization method using Darcy's law. This equation describes the flow of a fluid through a porous medium and has been previously presented to validate theoretical values of permeability in a micropatterned biopolymer scaffold.²⁰ This equation expresses permeability as a function of the flow rate Q (m^3/s) and pressure drop ΔP across a matrix:

$$k = \frac{QL\mu}{A\Delta P} \quad (1)$$

where A is the scaffold area (m^2), L is the matrix thickness (m), and μ is the solutions dynamic viscosity ($\text{Pa} \cdot \text{s}$). Pressure was monitored using a pressure transducer immediately downstream from the bioreactor. A similar system was

reported to assess the permeability of the subsynovial connective tissue and cell layer permeability.^{21,22}

Histological analysis

After decellularization, 5-mm ringlets were dissected from the vessels, leaving 10 mm from each end to avoid end effects. Samples were then fixed in a 10% buffered formalin solution overnight. Samples were then dehydrated in graded ethanol (80%, 95%, and 100% vol/vol) for 15 min (2×), and then embedded in paraffin and sectioned using standard protocols. Samples were stained using hematoxylin 7211 (Richard-Allan Scientific, Kalamazoo, MI) and counterstained with Eosin-Y (Richard-Allan Scientific-Kalamazoo, MI). Stained sections were observed using a Nikon Eclipse E800 epifluorescent microscope, and images were taken with an integrated digital camera (DXM1200F; Nikon, Tokyo, Japan).

SEM analysis

Decellularized and rinsed HUV samples were opened longitudinally to form a flat sheet, and dissected into 5×5 mm sections. Tissue sections were fixed in 1% (v/v) glutaraldehyde (Sigma, St. Louis, MO) for 4 h and then washed in PBS thrice for 5 min each. This was followed by a treatment of 1% osmium in PBS for 2 h to fix lipids. Samples were then progressively dehydrated in graded ethanol (30%, 50%, 70%, 90%, 95%, and 100%, v/v) for 10 min each. Critical point drying was carried out in carbon dioxide (Autosamdri-814; Tousimis, Rockville, MD). Samples were then gold sputtered and analyzed using a Jeol LSM-880 SEM at 15 kV.

Tensile testing

Analysis of the materials tensile properties was carried out at room temperature using a uniaxial tensile testing rig (Model SSTM-2K; United Testing Systems, Flint, MI). After decellularization was completed HUV scaffolds were rinsed with PBS and cut into 5-mm-wide ringlets. Tissue specimens ($n=9$) were loaded using stainless steel L-shaped hooks. Stress was applied in circumferential direction; specimens were first preloaded to a stress of 0.005 N at a rate of 5 mm/min and then elongated until failure, with force and extension recorded over time. Stress was calculated as the applied force over the cross sectional area. The elastic modulus was calculated from the slope of the linear section of the stress-strain graph.

All analytical methods were conducted at room temperature (21°C) unless otherwise stated. Data were reported as the average value ± standard error unless otherwise stated. Paired, two-tailed Student tests were performed to determine if mechanical properties and cellular marker extraction were statistically different (<0.05) between the groups.

Results

Phospholipids extraction

In all decellularization models, the majority of phospholipids extraction occurred after 3 h followed by a reduced extraction over time. With all convective flow pressures (5, 50, and 150 mmHg), the total amount of extracted phospholipids was at least twice that of rotary agitation (see

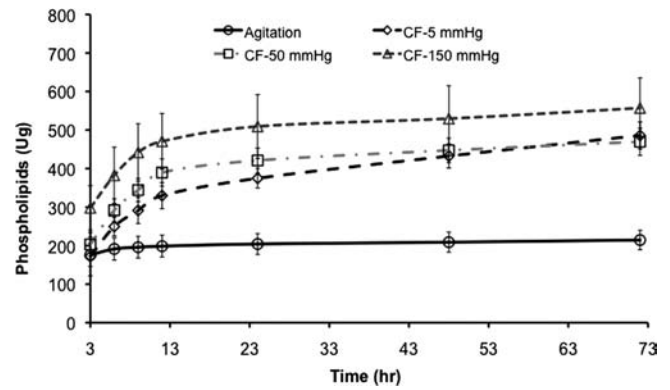


FIG. 3. Cumulative phospholipids extraction: comparative analysis between agitation and CF methodologies. Phospholipids extraction for all convective flow methods was higher than conventional agitation, with the highest extraction achieved with a transmembrane pressure differential of 150 mmHg.

Fig. 3). After 3 h, at luminal pressures of 150 mmHg, 1.4 times more phospholipid was extracted using the convective flow method than the total extracted with the agitation method over the entire 72 h extraction period ($298.0 \pm 57.73 \mu\text{g}$ and $176.0 \pm 29.9 \mu\text{g}$, respectively). Under these conditions a further $40 \mu\text{g/h}$ of phospholipids was extracted compared to agitation in the first 3 h. Similarly, at each time period after 6 h, the use of 5 and 50 mmHg luminal pressures in the HUV samples resulted in significantly higher extractions than traditional rotary agitation methods. As shown in Figure 4, cumulative phospholipid extraction at 150 mmHg was higher than that at 5 and 50 mmHg, as well as rotary agitation. The total extracted phospholipids using 150 mmHg pressure ($557.0 \pm 45.35 \mu\text{g}$) was equivalent to a 2.6-fold increase compared to rotary agitation at $214.6 \pm 14.62 \mu\text{g}$.

Soluble protein extraction

Comparative analysis of soluble protein extraction showed all convective flow methods extracted more soluble protein than rotary agitation decellularization. Two different trends of protein extraction were identified: agitation, medium (50 mmHg), and low pressures (5 mmHg) all showed an ini-

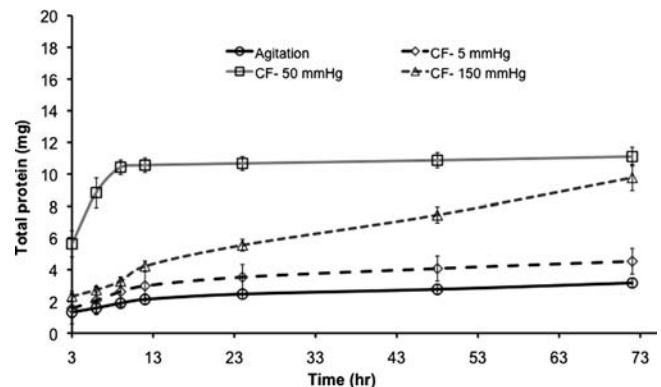


FIG. 4. Cumulative total protein extraction: protein extracted using pressure-based transmural flow was greater than conventional agitation, with the highest extraction rates at 50 mmHg.

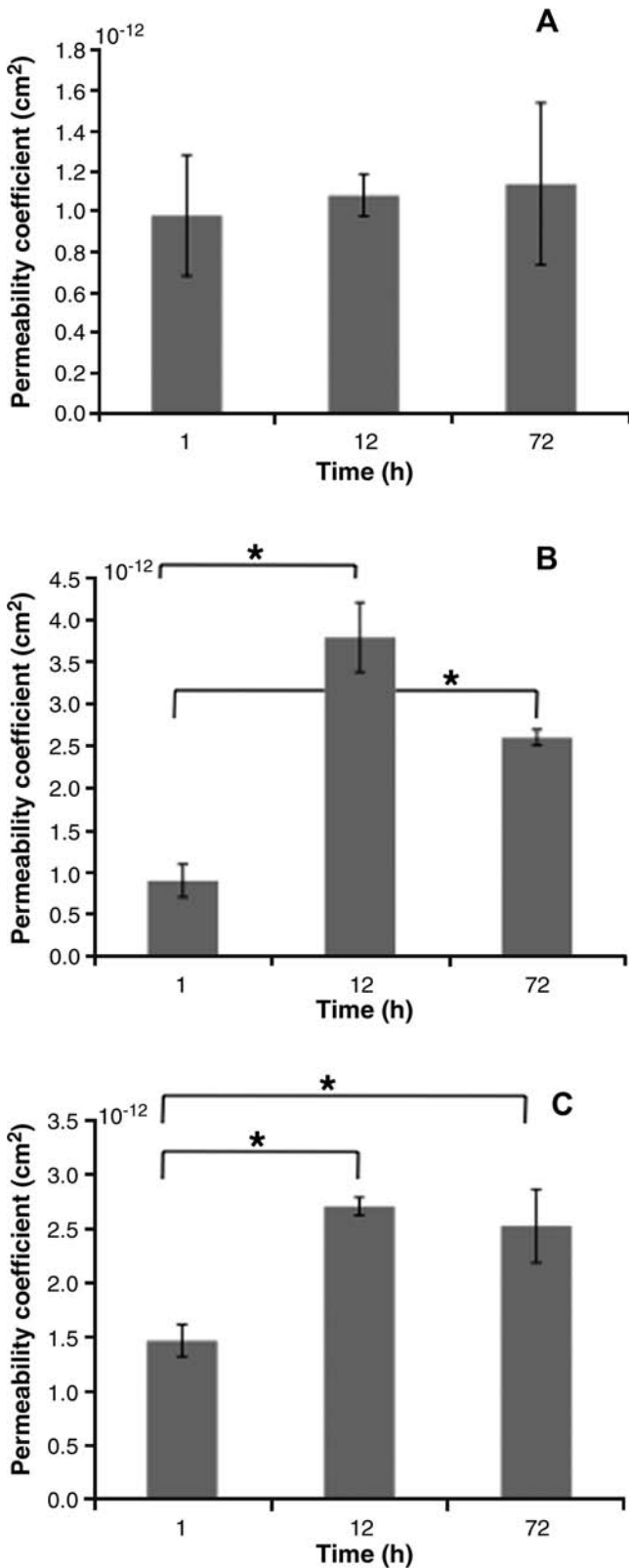


FIG. 5. Permeability coefficient: comparison of the matrix permeability calculated using Darcy's law throughout the decellularization process (A) 5 mmHg, (B) 50 mmHg, and (C) 150 mmHg. No significant difference was found for 5 mmHg, whereas permeability for 50 and 150 mmHg was significantly higher over time. *Denotes statistical significance.

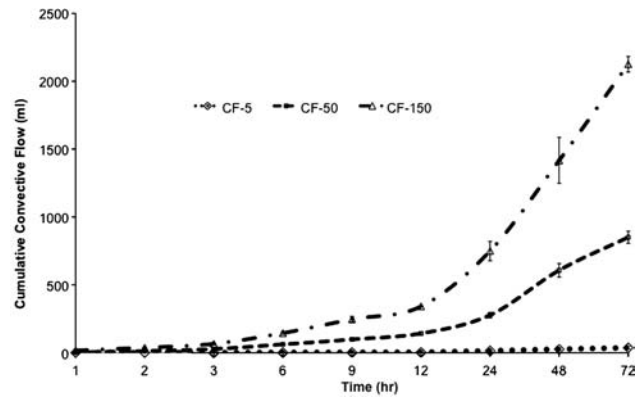


FIG. 6. Transmural flow. Higher pressures resulted in a progressive increase in transmural flow.

tial increase in protein extraction, followed by a plateau until experiment termination (see Fig. 4). Although the total protein extraction at 72 h at pressures of 50 and 150 mmHg was very similar, extraction at 150 mmHg took the total 72 h to extract amounts that were achieved in shorter periods of time at 50 mmHg pressure. These results indicate that medium pressure (50 mmHg) was the most efficient at extracting soluble proteins from HUV scaffold, removing in the first 3 h of treatment over four times the soluble proteins extracted with agitation (5.63 ± 0.83 and 1.32 ± 0.35 mg). Analysis of extraction at each time interval indicated that up to 6 h, medium pressure extracted significantly higher concentrations than either low or high pressure, as well as agitation ($p < 0.05$). At 12 h, the protein extracted with medium pressure (50 mmHg) decreased reaching a plateau (0.16 ± 0.05 mg), whereas at the same time point, higher pressure at 150 mmHg extraction increased steadily over the remaining 60 h. The overall extraction of protein was 3.5 times higher with the medium pressure than with agitation at 72 h (11.1 ± 0.07 compared to 3.1 ± 0.06 mg).

Permeability

Permeability of the HUV was calculated over time for each pressure, using a mean thickness value of $0.75 \mu\text{m}$ and Equation (1). The permeability coefficient profile is represented in Figure 5. The average permeability coefficients were $1.1 \pm 0.5 \times 10^{-12} \text{ cm}^2$ at 5 mmHg, $2.8 \pm 0.9 \times 10^{-12} \text{ cm}^2$ at 50 mmHg, and $2.3 \pm 0.5 \times 10^{-12} \text{ cm}^2$ at 150 mmHg. The permeability coefficient remained unchanged over time for the low-pressure convective flow (5 mmHg), whereas under medium and high pressures, the permeability was significantly higher after 12 and 72 h. The average transmural flow rate was significantly higher with higher transmembrane pressures (0.42 ± 0.2 , 11.25 ± 1.9 , and $27.69 \pm 4.2 \text{ mL/h}$ for low, medium, and high pressures, respectively). In addition, higher pressures yielded cumulative transmural flow significantly higher than low pressure (36.9 ± 8.8 , 850.8 ± 43.9 , and $2125.7 \pm 57.7 \text{ mL}$ with low, medium, and high pressures; see Fig. 6).

Mechanical properties

As shown in Figure 7, the characteristic stress-strain relationship for connective tissue was preserved after decellularization (both agitation and convective flow). The profile

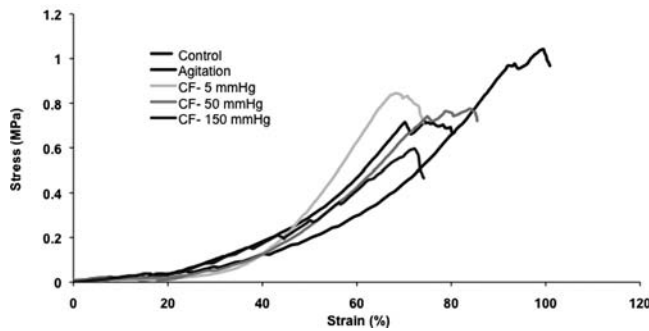


FIG. 7. Representative stress–strain analysis. The biphasic stress–strain relationship seen in native blood vessels was retained, with the characteristic toe region observed for all decellularization methods, although a shift in strain is noted at 150 mmHg.

displays a toe region followed by a linear portion until tissue failure. Mechanical properties of the acellular HUV were compared to control tissue and are summarized in Table 1. Modulus of elasticity and ultimate tensile strength for all decellularized tissues (rotary agitation and convective flow methods) were not statistically different from controls ($p > 0.05$). However, the Young's modulus and ultimate tensile strength were significantly lower for high pressure (150 mmHg) than for medium pressure (50 mmHg) (see Fig. 8). The tubular structure of the decellularized HUV was maintained after the convective flow method, whereas the tissue decellularized by the agitation method was shown to soften and loose rigidity (see Fig. 9).

HYP quantification

HYP, a unique amino acid in collagen, was used as an indirect marker of the collagen degradation that may result from the treatment processes. Figure 10 shows the HYP content within the decellularization solution, with HYP levels significantly lower with the convective methods than agitation. However, the concentration detected with rotary agitation was as low as 0.6% of the total HYP content in the HUV before treatment ($21.2 \pm 3.9 \mu\text{g}$ compared to $3.4 \pm 0.4 \text{ mg}$), indicating a very small fraction of the total content. HYP concentration was $21.2 \pm 3.9 \mu\text{g/mL}$ in agitation, compared to 11.5 ± 4.1 , 13.1 ± 3.0 , and $4 \pm 0.1 \mu\text{g/mL}$ in low (5 mmHg), medium (50 mmHg), and high (150 mmHg) pressures, respectively.

TABLE 1. ULTIMATE TENSILE STRENGTH

Sample description	Maximum load (N)	Ultimate tensile strength (MPa)
Cellular control	13.69 ± 3.79	0.78 ± 0.22
Agitation decellularization	16.06 ± 2.48	0.92 ± 0.14
Convective flow (5 mmHg)	13.02 ± 1.61	0.74 ± 0.09
Convective flow (50 mmHg)	16.08 ± 2.81	$0.92 \pm 1.61^*$
Convective flow (150 mmHg)	11.67 ± 1.93	$0.67 \pm 0.11^*$

No evident change in the ultimate tensile strength was determined with the different applied transmembrane pressures. The lowest value was found for the high-pressure bioreactor samples.

*Denotes statistically significant difference from controls.

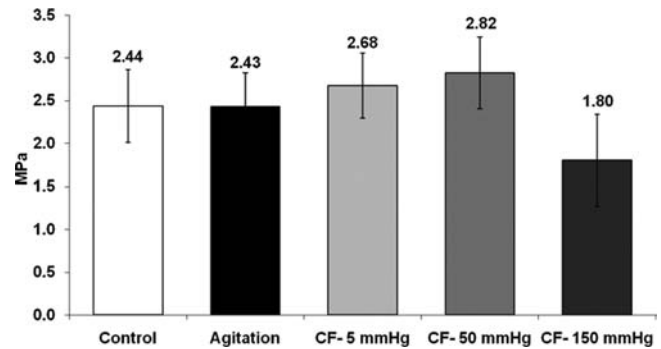


FIG. 8. Elastic modulus. Modulus was obtained from the linear region of the strain–stress curves after mechanical testing. The modulus of the acellular HUV was compared with control tissue. Elasticity was found to decrease significantly with pressure at 150 mmHg compared to 50 mmHg.

SEM and histology

Images from the histological analysis have shown the general structure of the circumferential collagen fibers to be preserved after all methods of decellularization. SEM analysis of convectively decellularized HUVs luminal surface displayed a partially disrupted basement membrane at higher pressures, whereas agitation methods showed a smoother, more uniform surface structure (see Fig. 11). Cellular debris remained in the medial layer of the HUV when treated by rotary agitation; by contrast, samples that underwent convective flow decellularization (5 and 50 mmHg) were void of cells. However, at 150 mmHg cells were observed within the media layer of the vessel wall (see Fig. 12).

Discussion

The goal of these investigations was to assess the effectiveness of a convective flow–based decellularization method for preparing *ex vivo* scaffolds for tissue engineering applications. Although decellularization of tissues focuses on the extraction of cellular markers, such as lipids and soluble proteins, other parameters must also be considered. Structure–function of *ex vivo* tissues is a key property that sets these materials apart from current synthetics, and the ability of the decellularization process to maintain the tissues original structure and biomechanics is also important. In addition, the time taken to complete this process can have a significant commercial impact; that is, faster and more effective processing reduces production, and hence patient costs. To achieve this, a modified vascular perfusion bioreactor and process flow circuit was adapted such that solvent could be perfused through the lumen (tube-side) of the vessel at an elevated pressure relative to abluminal (shell-side) of the bioreactor. This produced a uniform convective flow, or transmural flux, passing through the vessel wall to enhance the decellularization process.

A diverse range of tissue types and chemical treatments have been used with agitation-based methods, where the tissue is submerged in different chemical and/or enzymatic solutions and then agitated, typically by shaking, or rotating either in stationary bottles, or roller bottles.^{9,15,23–28} Human saphenous veins have been decellularized by placing the specimens in a 37°C sodium dodecyl sulfate (SDS) solution

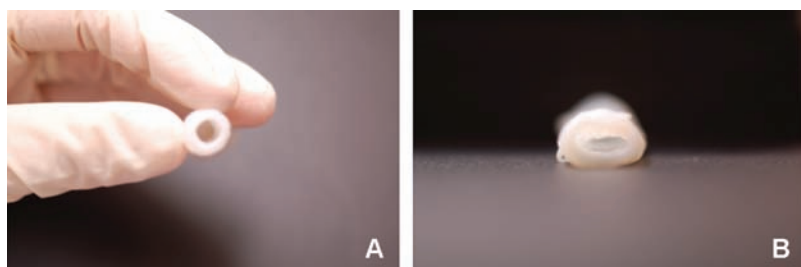


FIG. 9. Representative images of decellularized HUv after (A) convective flow method and (B) agitation. The samples treated with convective flow conserved the cylindrical structure of native tissue, while the agitation method was shown to soften and loose rigidity. Color images available online at www.liebertonline.com/ten.

within a shaking bath for 15 h followed by a rinsing in PBS.²⁹ Following similar technologies, others have produced acellular liver stroma,⁸ rat aortic valve,^{24,26} and iliac artery.³⁰ Although the molecular details are not clear, some methods are more effective than others. For example, only partial decellularization was achieved when porcine heart valves were treated under continuous agitation in a 0.05% trypsin solution for <24 h followed by a 24 h PBS washing step.¹¹ Although, this maybe more a function of the specific chemistry than the method of agitation. Agitation decellularization relies on the diffusion of the solvent through the sample, which is limited by the density of the ECM and its thickness. As a consequence mass transfer issues arise limiting the effectiveness of the process. Collagen–elastin matrices prepared from canine blood vessels (arteries and veins) and processed under alkaline conditions showed that the femoral iliac arteries were more resistant to the treatment than the thinner walled veins, which retained some of the smooth muscle cells after 48 h of treatment. By contrast, thinner walled veins were depleted of cells after 18 h of treatment. Extended treatment times achieved complete cellular removal in the arteries; however, increased ECM fragmentation occurred, with a significant reduction in collagen content.⁹ More recently, decellularization approaches have incorporated perfusion bioreactors or a modified Langendorff apparatus, to produce acellular matrices. Karim *et al.* constructed a heart valve reactor where tissue was immersed in a trypsin/EDTA solution and continuously rotated for 24 h (37°C and pH 7.2), followed by a PBS treatment at a perfusion rate of 18.8 mL/min.¹⁶ Optimized conditions lead to a

complete removal of porcine cells; however, reduced cell extraction was noted when lower rates of rotation or perfusion were used and/or decreased time frames. In other investigations, whole rat hearts were successfully decellularized by perfusion of a 1% SDS solution over a 12 h period under a mean coronary perfusion pressure of 74 mmHg.

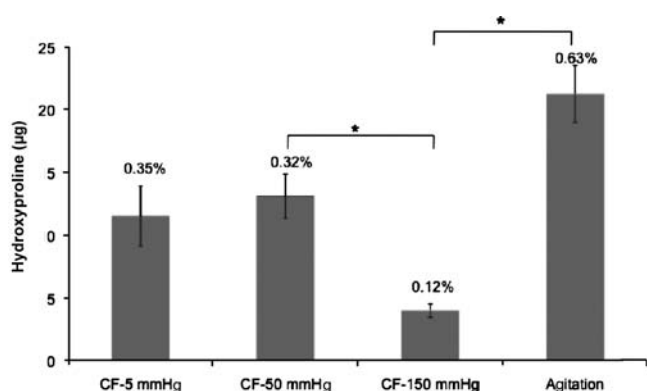


FIG. 10. Scaffold deterioration measured by assessing free HYP. Percent values indicate the HYP fraction compared to native HYP content. Agitation decellularization had increased concentrations of soluble HYP than the convective flow methods. *Shows statistically different data sets.

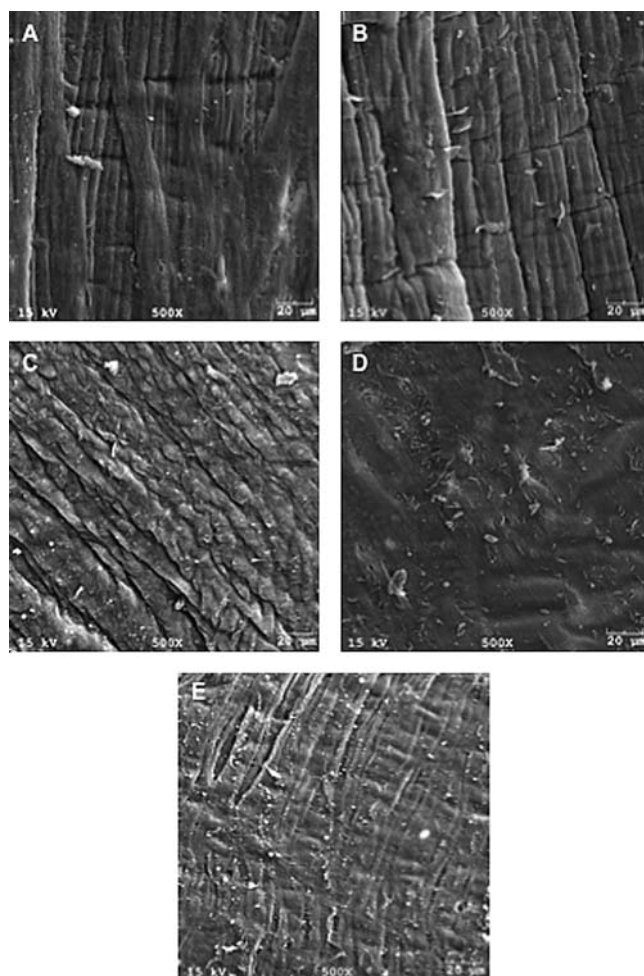
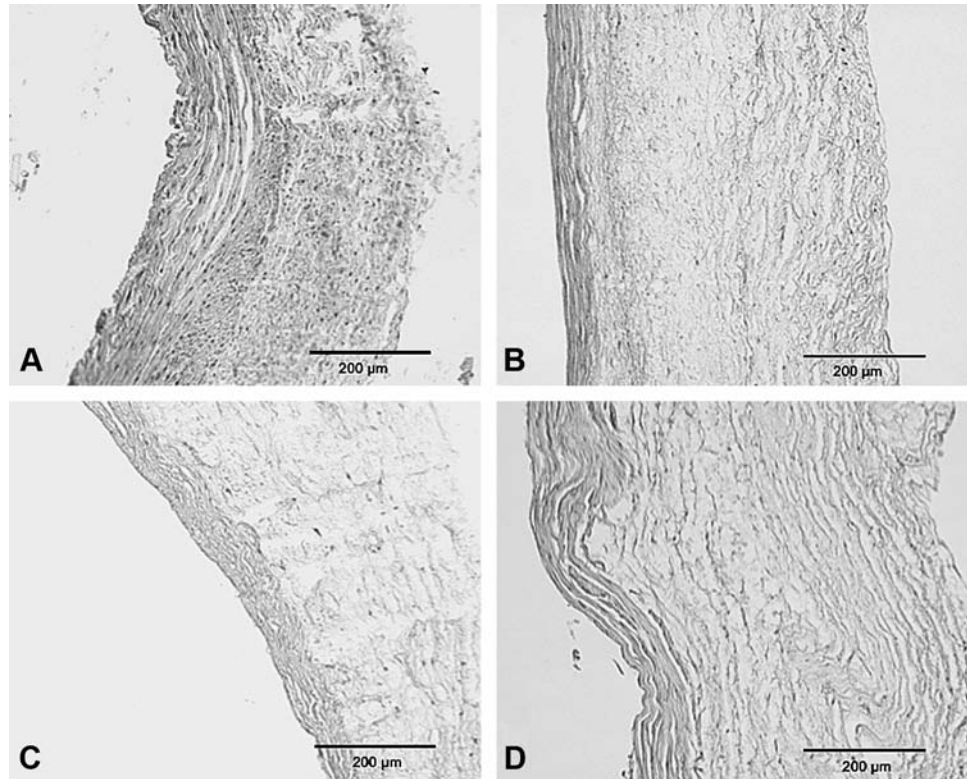


FIG. 11. SEM images of the luminal surface. Native cellular tissue and samples decellularized by agitation show the natural structure of the elastic lamina. The convoluted structure of the luminal surface deteriorated as the applied pressure in the system increases. Disruption of basal membrane was observed when high pressure was used. (A) Native tissue, (B) agitation decellularization, (C) CF-5 mmHg, (D) CF-50 mmHg, and (E) CF-150 mmHg. All lumen sides were observed cell free.

FIG. 12. Bright field microscopy. The acellular HUV after (A) agitation, and convective flow using three different pressures (B) 5 mmHg, (C) 50 mmHg, and (D) 150 mmHg. The agitation method was shown to be positive for cell nuclei and a mild separation of the collagen fibers.



DAPI stain revealed no intact cell nuclei after perfusion decellularization; additionally, ECM components, collagen I and III, fibronectin, and laminin were preserved. The aortic wall and aortic valve leaflet fiber orientation was also conserved, and the valve remained patent after the constant coronary pressure throughout the perfusion decellularization process.¹⁷

Assessment of phospholipids is important not only as a marker for cell extraction and hence improved immunocompatibility, but also because retained lipids have been shown to result in tissue calcification. Investigations have shown that removal of lipids with either chloroform/methanol, SDS, or EtOH resulted in reduced calcification.³¹ The convective flow method assessed here was shown to be significantly more effective at removing lipid than the agitation method, with the higher transmembrane pressure differential (150 mmHg) being more effective than the lower pressures (5 and 50 mmHg). Due to the chemistry of the phospholipid molecules, relative to proteins, these molecules are more easily solubilized by the acetone/EtOH solution and removed from the interstitial fibers by the convective flow. Ethanol's properties reside in the presence of its hydroxyl group and its short carbon chain. Its polar nature makes ethanol soluble with many other organic compounds, while the nonpolar carbon chain gives it the property of dissolving nonpolar substances such as lipids.³² Further, ethanol has been investigated as a treatment to remove residual surfactant after tissue processing^{12,25} as well as a tissue preservative.⁹ EtOH has also been shown to reduce calcification of prosthetic heart valves when used as a treatment before decellularization.^{31,32}

The acetone/EtOH decellularization solution used in these investigations was selected over arguably more effective

combined treatments because of their effectiveness at solubilizing lipids, and also to allow the use of enzyme-based assays for lipid analysis. Importantly, the objective of this study was to investigate the effectiveness of a pressure-based system versus the shaking bath method typically used to decellularize tissue. Irrespective of the effectiveness of a specific lipid solubilization treatment, the physical method of applying a defined pressure, as described here, was significantly more effective at lipid removal compared to agitation only. Remaining soluble proteins or cellular debris can also elicit an immune response; therefore, it is desirable to extract as many of these components as possible to minimize graft rejection. The extraction of soluble protein was not as predictable as the phospholipids. Convective flow at 50 mmHg resulted in a more efficient removal of soluble proteins than other treatments. After the first 3 h at 50 mmHg two- to threefold increases in total protein extraction was observed over all other extraction processes, with less damage to structural collagen, as shown by HYP quantification with the agitation method. Contrary to the effect of higher pressures being more effective at phospholipid extraction, higher pressure protein removal at 150 mmHg displayed lower extraction over the first 6 h than at 50 mmHg. A plausible explanation for this mechanism is that higher constant pressures result in a compaction of the vessel wall, effectively reducing the porosity. That combined with the chemical nature of the solvent that precipitates soluble proteins results in a clogging effect that reduces outflow. Over time, as the protein and other soluble component are extracted, permeability increases and allows these larger aggregates to be pushed out of the scaffold, as observed with a progressive increase in protein extraction over the time course.

HYP has been widely used as a distinctive marker of collagen content. HYP is produced after hydrolysis of proline residues within the collagen sequence and can be used for quantification purposes. As such, the level of collagen degradation can be determined by measuring the concentration of free HYP in solution after the decellularization process. Although the concentration of HYP detected in the solution was significantly higher in agitation decellularization, this represents a small fraction (0.6% of the total average HYP content) of tissue before treatment. It is hypothesized that structural collagen was damaged (releasing HYP) during agitation as vessels were bent and kinked during the agitation process, while in the perfusion bioreactor they remained as cylindrical structures.

The permeability coefficient of the HUV was affected by each of the three pressure gradients evaluated. The continuous extraction of phospholipids and other soluble components will increase the tissues porosity resulting in typically higher permeability values. However, between 12 and 72 h a leveling off or reduction in permeability coefficient was shown. It is hypothesized that this was caused by the higher pressure gradients compacting the fibers as well as the potential of the larger proteins or protein aggregates to block scaffold pores, and therefore increasing the resistance of the convective flow.²¹ Other investigations have reported values of permeability related to the transmembrane pressure differential. For example, the intrinsic permeability of sub-synovial connective tissue in the human carpal tunnel was reported to be $0.89 \pm 0.93 \times 10^{-14} \text{ m}^4/\text{N s}$ at 96.5 kPa and $1.04 \pm 1.54 \times 10^{-14} \text{ m}^4/\text{N s}$ at 68.9 kPa.²¹

Examination of the ECM revealed that the gross structure of collagen within the vein was conserved after both agitation and convective flow decellularization. The collagen fibers after convective flow treatment appeared to be loosely packed when compared to agitated samples. It is not clear what causes this effect, but it is possibly a result of the solution path through the vessel wall, or that the more effective removal of interstitial soluble ECM components results in the larger (insoluble) fibers spreading. The convective flow model resulted in scaffolds void of endothelial cells and of the majority of smooth muscle cells from the tunica media, whereas cells were present throughout the medial layer of scaffolds exposed to standard agitation.

Adequate strength to withstand physiological forces is a requirement for any tissue graft, and as such the effects of tissue processing is an important consideration. In these investigations static tensile testing was performed as an indicator of these changing properties. Although dynamic analysis is more effective to assess the active conditions that blood vessels are normally exposed to, static analysis provides a useful marker of variation between control and test groups. Results showed that the applied pressure during the convective flow decellularization process had no detectable negative effect on the ECM. No statistical difference was noted with the modulus of elasticity and maximum strength between controls and treated tissue. Interestingly, although the mechanical properties of the scaffold were not changed, scaffolds exposed to the convective decellularization retained their cylindrical shape. These appear contradictory results, but are likely to be caused by the ECM fibers in the veins exposed to agitation to lose their native alignment resulting in less structural rigidity at low pressure. There may also

be a very mild cross-linking effect that may aid this shape retention. As a consequence, the graft will have improved surgical handling characteristics.³²

The potential of the convective flow as a mechanism of tissue decellularization was assessed and has been demonstrated to be significantly more effective than traditional rotary agitation methods. Although specific epitope retention was not addressed in these investigations, future studies will assess specific markers using immunohistochemistry to colocalize targeted molecules, as well as any variation in distribution that may exist. Further, the ultimate effectiveness of any decellularization method requires *in vivo* testing to determine immunological responses. Although other, perhaps more effective agents to decellularize the tissue can be used, the principle of an applied pressure has been demonstrated. Moreover, due to the increased efficiency of the uniform pressure-based system, less aggressive agents can be used that achieve the same level of decellularization. The convective flow approach also significantly reduces processing times, which is an important factor in any processing system. This is particularly important with FDA regulations that require tissue samples to be processed as a single unit, rather than the batch processing typically used in laboratory agitation methods. This approach can also be used to develop multistep processes that can be housed within a single bioreactor to decellularize, seed, and culture re-cellular constructs. By improving process efficiency within a single system, development lead times can be reduced, while minimizing graft handling before clinical use.

Disclosure Statement

No competing financial interests exist.

References

- Hodde, J. Naturally occurring scaffolds for soft tissue repair and regeneration. *Tissue Eng* **8**, 295, 2002.
- Gilbert, T.W., Sellaro, T.L., and Badylak, S.F. Decellularization of tissues and organs. *Biomaterials* **27**, 3675, 2006.
- Booth, C., Korossis, S.A., Wilcox, H.E., Watterson, K.G., Kearney, J.N., Fisher, J., and Ingham, E. Tissue engineering of cardiac valve prostheses I: development and histological characterization of an acellular porcine scaffold. *J Heart Valve Dis* **11**, 457, 2002.
- Badylak, S.F. Xenogeneic extracellular matrix as a scaffold for tissue reconstruction. *Transpl Immunol* **12**, 367, 2004.
- Knight, R.L., Wilcox, H.E., Korossis, S.A., Fisher, J., and Ingham, E. The use of acellular matrices for the tissue engineering of cardiac valves. *Proc Inst Mech Eng [H]* **222**, 129, 2008.
- Wang, X., Lin, P., Yao, Q., and Chen, C. Development of small-diameter vascular grafts. *World J Surg* **31**, 682, 2007.
- Schmidt, C.E., and Baier, J.M. Acellular vascular tissues: natural biomaterials for tissue repair and tissue engineering. *Biomaterials* **21**, 2214, 2000.
- Brown, B., Lindberg, K., Reing, J., Stolz, D.B., and Badylak, S.F. The basement membrane component of biologic scaffolds derived from extracellular matrix. *Tissue Eng* **12**, 519, 2006.
- Goissis, G., Suzigan, S., Parreira, D.R., Maniglia, J.V., Braile, D.M., and Raymundo, S. Preparation and characterization of collagen-elastin matrices from blood vessels intended as small diameter vascular grafts. *Artif Organs* **24**, 217, 2000.

10. Kasimir, M.T., Rieder, E., Seebacher, G., Silberhumer, G., Wolner, E., Weigel, G., and Simon, P. Comparison of different decellularization procedures of porcine heart valves. *Int J Artif Organs* **26**, 421, 2003.
11. Schenke-Layland, K., Vasilevski, O., Opitz, F., Konig, K., Riemann, I., Halbhuber, K.J., Wahlers, T., and Stock, U.A. Impact of decellularization of xenogeneic tissue on extracellular matrix integrity for tissue engineering of heart valves. *J Struct Biol* **143**, 201, 2003.
12. Gratzner, P.F., Harrison, R.D., and Woods, T. Matrix alteration and not residual sodium dodecyl sulfate cytotoxicity affects the cellular repopulation of a decellularized matrix. *Tissue Eng* **12**, 2975, 2006.
13. Brown, A.L., Brook-Allred, T.T., Waddell, J.E., White, J., Werkmeister, J.A., Ramshaw, J.A., Bagli, D.J., and Woodhouse, K.A. Bladder acellular matrix as a substrate for studying *in vitro* bladder smooth muscle-urothelial cell interactions. *Biomaterials* **26**, 529, 2005.
14. Freytes, D.O., Badylak, S.F., Webster, T.J., Geddes, L.A., and Rundell, A.E. Biaxial strength of multilaminated extracellular matrix scaffolds. *Biomaterials* **25**, 2353, 2004.
15. Lin, P., Chan, W.C., Badylak, S.F., and Bhatia, S.N. Assessing porcine liver-derived biomatrix for hepatic tissue engineering. *Tissue Eng* **10**, 1046, 2004.
16. Karim, N., Golz, K., and Bader, A. The cardiovascular tissue-reactor: a novel device for the engineering of heart valves. *Artif Organs* **30**, 809, 2006.
17. Ott, H.C., Matthiesen, T.S., Goh, S.K., Black, L.D., Kren, S.M., Netoff, T.I., and Taylor, D.A. Perfusion-decellularized matrix: using nature's platform to engineer a bioartificial heart. *Nat Med* **14**, 213, 2008.
18. Daniel, J., Abe, K., and McFetridge, P.S. Development of the human umbilical vein scaffold for cardiovascular tissue engineering applications. *Asaio J* **51**, 252, 2005.
19. Inayama, S., Shibata, T., Ohtsuki, J., and Saito, S. A new microanalytical method for determination of hydroxyproline in connective tissues. *Keio J Med* **27**, 43, 1978.
20. Figallo, E., Flaibani, M., Zavan, B., Abatangelo, G., and Elvassore, N. Micropatterned biopolymer 3D scaffold for static and dynamic culture of human fibroblasts. *Biotechnol Prog* **23**, 210, 2007.
21. Osamura, N., Zhao, C., Zobitz, M.E., An, K.N., and Amadio, P.C. Permeability of the subsynovial connective tissue in the human carpal tunnel: a cadaver study. *Clin Biomech (Bristol, Avon)* **22**, 524, 2007.
22. Chandra, A., Barillas, S., Suliman, A., and Angle, N. A novel fluorescence-based cellular permeability assay. *J Biochem Biophys Methods* **70**, 329, 2007.
23. Amiel, G.E., Komura, M., Shapira, O., Yoo, J.J., Yazdani, S., Berry, J., Kaushal, S., Bischoff, J., Atala, A., and Soker, S. Engineering of blood vessels from acellular collagen matrices coated with human endothelial cells. *Tissue Eng* **12**, 2355, 2006.
24. Grauss, R.W., Hazekamp, M.G., van Vliet, S., Gittenberger-de Groot, A.C., and DeRuiter, M.C. Decellularization of rat aortic valve allografts reduces leaflet destruction and extracellular matrix remodeling. *J Thorac Cardiovasc Surg* **126**, 2003, 2003.
25. Malone, J.M., Brendel, K., Duhamel, R.C., and Reinert, R.L. Detergent-extracted small-diameter vascular prostheses. *J Vasc Surg* **1**, 181, 1984.
26. Meyer, S.R., Chiu, B., Churchill, T.A., Zhu, L., Lakey, J.R., and Ross, D.B. Comparison of aortic valve allograft decellularization techniques in the rat. *J Biomed Mater Res A* **79**, 254, 2006.
27. Wilson, G.J., Yeger, H., Klement, P., Lee, J.M., and Courtman, D.W. Acellular matrix allograft small caliber vascular prostheses. *ASAIO Trans* **36**, M340, 1990.
28. McFetridge, P.S., Daniel, J.W., Bodamyali, T., Horrocks, M., and Chaudhuri, J.B. Preparation of porcine carotid arteries for vascular tissue engineering applications. *J Biomed Mater Res* **70A**, 224, 2004.
29. Schaner, P.J., Martin, N.D., Tulenko, T.N., Shapiro, I.M., Tarola, N.A., Leichter, R.F., Carabasi, R.A., and Dimuzio, P.J. Decellularized vein as a potential scaffold for vascular tissue engineering. *J Vasc Surg* **40**, 146, 2004.
30. Borschel, G.H., Huang, Y.C., Calve, S., Arruda, E.M., Lynch, J.B., Dow, D.E., Kuzon, W.M., Dennis, R.G., and Brown, D.L. Tissue engineering of recellularized small-diameter vascular grafts. *Tissue Eng* **11**, 778, 2005.
31. Jorge-Herrero, E., Fernandez, P., Gutierrez, M., and Castillo-Olivares, J.L. Study of the calcification of bovine pericardium: analysis of the implication of lipids and proteoglycans. *Biomaterials* **12**, 683, 1991.
32. Vyavahare, N., Hirsch, D., Lerner, E., Baskin, J.Z., Schoen, F.J., Bianco, R., Kruth, H.S., Zand, R., and Levy, R.J. Prevention of bioprosthetic heart valve calcification by ethanol preincubation: efficacy and mechanisms. *Circulation* **95**, 479, 1997.

Address reprint requests to:

Peter S. McFetridge, Ph.D.

School of Chemical, Biological, and Materials Engineering

University of Oklahoma

100 E Boyd

Norman, OK 73019-1004

E-mail: pmcfetridge@ou.edu

Received: July 2, 2008

Accepted: October 21, 2008

Online Publication Date: January 9, 2009